Three-dimensional active earth pressures

Abdul-Hamid Soubra, Didier Galvani, Pierre Regenass

European Congress on Computational Methods in Applied Sciences and Engineering
ECCOMAS 2000
Barcelona, 11-14 September 2000

THREE-DIMENSIONAL ACTIVE EARTH PRESSURES

Abdul-Hamid Soubra*, Didier Galvani*, and Pierre Regenass*

Ecole Nationale Supérieure des Arts et Industries de Strasbourg
24, Bld de la Victoire
67084 Strasbourg cedex
France
e-mail: Ahamid.Soubra@ensais.u-strasbg.fr, Pierre.Regenass@ensais.u-strasbg.fr

Key words: Active pressure, limit analysis

Abstract. A theoretical approach to evaluate the active earth pressures taking into account the three-dimensional effect is presented. The analysis considers the general case of a frictional and cohesive (c, ϕ) soil subjected to a vertical surcharge loading q acting on the ground surface. This approach is based on the kinematical method of the limit analysis theory. A translational soil-wall movement is considered in the present analysis. A three-dimensional kinematically admissible failure mechanism *M1,* composed of a single rigid block is proposed. This mechanism is an extension into three dimensions of the classical two-dimensional Coulomb mechanism. The three-dimensional active earth pressure coefficients $K_{a\gamma}$, K_{ac} and K_{aq} representing the effect of soil weight, cohesion and surcharge loading are obtained by numerical optimisation. The numerical results so obtained show the influence of the different geometrical and mechanical characteristics on the three-dimensional active earth pressures.

1 INTRODUCTION

The problem of the two-dimensional active earth pressures acting on rigid retaining structures has been widely studied by several investigators[1, 2, 3, 4]. The review of existing literature has shown that little attention is given to the *3-D* aspects. In this paper, a theoretical approach to evaluate the three-dimensional active earth pressures is presented. This approach is based on the kinematical method of the limit analysis theory. A three-dimensional kinematically admissible failure mechanism *M1* is proposed. The analysis considers the general case of a frictional and cohesive (c, ϕ) soil with an eventual surcharge loading q acting on the ground surface. The numerical results of the three-dimensional coefficients are presented and discussed.

2 THE UPPER AND LOWER-BOUND THEOREMS OF LIMIT ANALYSIS

As is well known, the limit theorems of the limit analysis theory enable us to determine upper and lower bound solutions for the stability problems of a rigid perfectly plastic material.

While the lower-bound method is complex due to the fact that it requires the construction of a complete stress field, the upper-bound method is simpler: Equating the rate of external work to the rate of internal energy dissipation for a kinematically admissible velocity field gives an unsafe solution of the collapse or limit load.

A kinematically admissible velocity field is one that satisfies the flow rule, the velocity boundary conditions and compatibility. During plastic flow, energy is dissipated by general plastic yielding of the soil mass, as well as by sliding along velocity discontinuities where jumps in the normal and tangential velocities may occur. Note that the velocity field at collapse is often modelled by a mechanism of rigid blocks that move with constant velocities. Since no general plastic deformation of the soil mass is permitted to occur, the energy is dissipated solely at the interfaces between adjacent blocks which constitute velocity discontinuities.

3 UPPER-BOUND APPROACH

It is well known that the three-dimensional nature of the active earth pressure problem has the favourable effect of decreasing the active earth pressures exerted on the wall. In this paper, the decrease of the active earth pressure coefficients due to the decrease of the wall breadth is investigated using the kinematical approach of the limit analysis theory.

3.1. Assumptions

The following assumptions have been made in the analysis:

1. The wall of dimensions bxh (b = breadth; h = height) is vertical and the backfill is horizontal;
2. A translational soil-wall movement is assumed;
3. The soil is homogeneous and isotropic. It is assumed to be an associated flow rule Coulomb material obeying Hill's maximal work principle;

4. The angle of friction δ at the soil-structure interface is assumed to be constant. This hypothesis is in conformity with the translational kinematics assumed in this paper;
5. A tangential adhesive force P_{ad} is assumed to act at the soil-structure interface. The intensity of this force is $c\dfrac{\tan\delta}{\tan\phi}bh$;

The velocity at the soil-structure interface is assumed to be tangential to the wall (see Chen [5]). Collins[6] and Mroz and Drescher[7] assumed that the interfacial velocity is inclined at δ to the wall in order to respect the normality condition. Both hypotheses lead to the same result of the limit load (see Drescher and Detournay[8], Michalowski[9] and Soubra[10]).

3.2. Failure mechanism

M1 is an extension into three dimensions of the classical two-dimensional Coulomb mechanism. This mechanism is translational and is composed of a single rigid block (Figure 1). It is limited by the lower plane *AA'D'D* and the two lateral planes *ABD* and *A'B'D'*. Two different cases may occur depending on the height to breadth ratio *h/b*. Figure 1 shows the failure mechanism for small *h/b* values (Case I) where the lateral planes do not intersect and figure (2) shows the second case where the lateral planes intersect along the vertical straight line *TT'*.

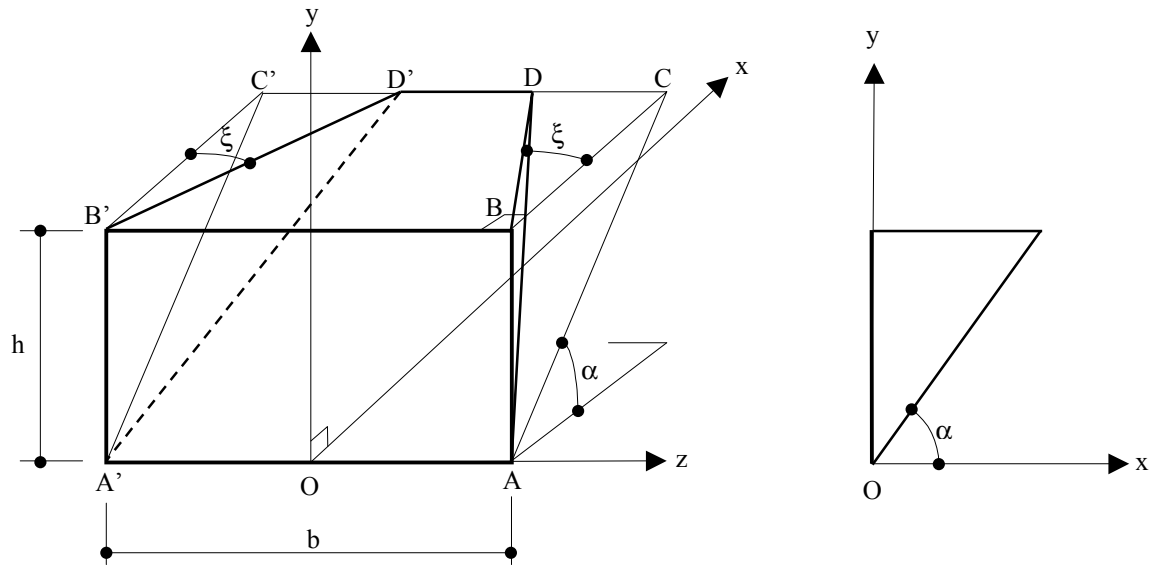

Figure 1: Failure mechanism *M1* for small *h/b* values (Case I)

For the case I, the soil mass *AA'BB'DD'* moves with velocity V_1 inclined at an angle of $\alpha-\phi$ to the horizontal direction (Fig. 3), the wall moves with velocity V_0 and $V_{0,1}$ represents the relative velocity at the soil-structure interface. All these velocities are parallel to the vertical symmetrical plane *xOy*. For the case II, the kinematics is similar to that of Case I.

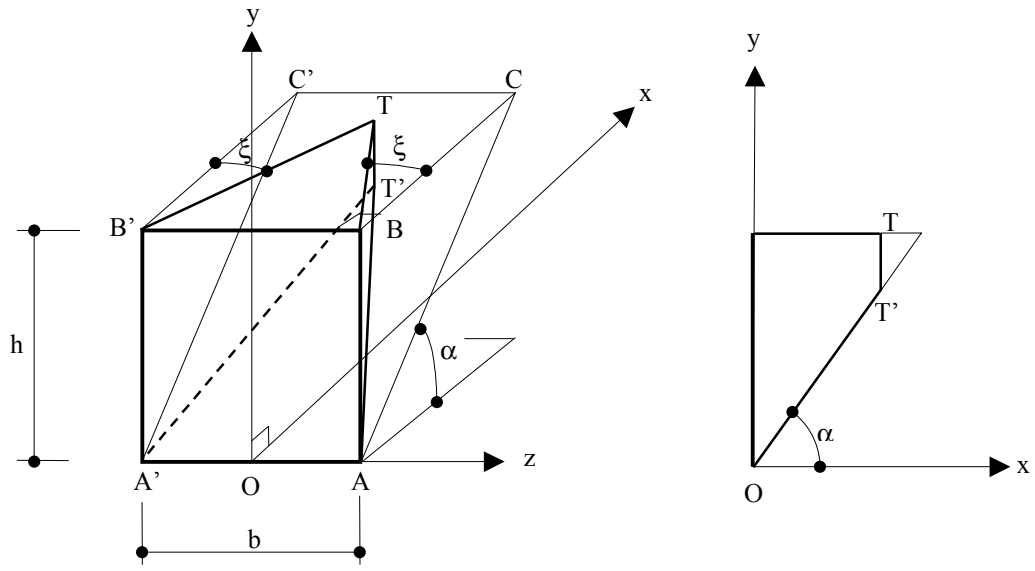

Figure 2: Failure mechanism *M1* for large *h/b* values (Case II)

Using the velocity hodograph shown in Fig. 3, we have:

$$V_1 = \frac{V_0}{\cos(\alpha - \phi)} \tag{1}$$

$$V_{0,1} = \tan(\alpha - \phi) V_0 \tag{2}$$

Note that the velocity V_1 should also make an angle ϕ with the lateral plane *ABD* (respectively *A'B'D'*) in order to respect the normality condition. This imposes that the angle between the vector V_1 and its orthogonal projection on the lateral plane *ABD* (respectively *A'B'D'*) must be equal to ϕ. This condition yields the orientation of the lateral planes *ABD* and *A'B'D'* for a given inclination α of the lower plane *AA'DD'*. It can be shown that the dihedral angle ξ [cf. Fig. 1] between the lateral plane *ABD* (respectively *A'B'D'*) and the vertical plane *xOy* can be expressed as

$$\tan\xi = \frac{\sin\phi}{\sqrt{\cos^2\phi - \sin^2(\alpha - \phi)}} \tag{3}$$

This mechanism is defined by a single angular parameter α, the dihedral angle between the lower plane *AA'D'D* and the horizontal plane.

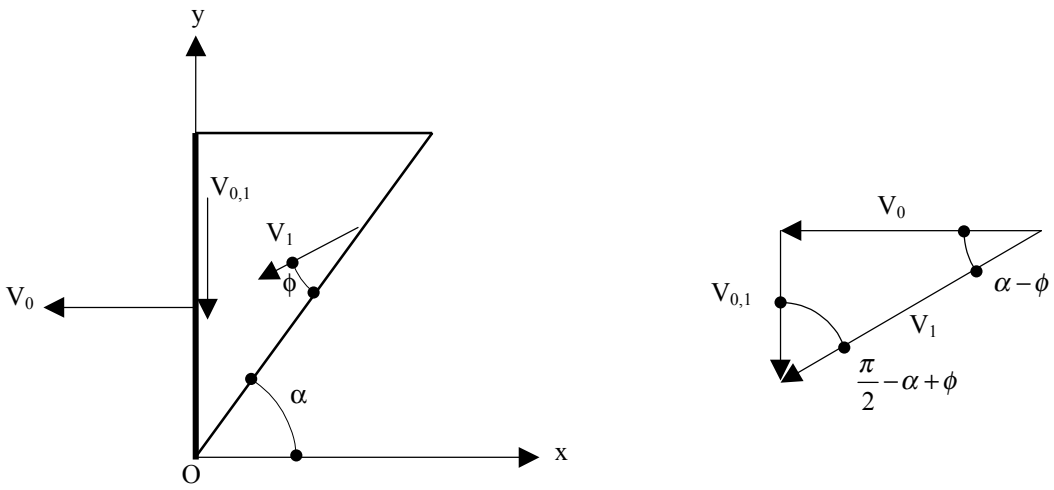

Figure 3: Velocity field and velocity hodographs (Case I)

3.3. Work equation

As shown in Figure (4), the external forces contributing to the rate of external work consist of the active earth force P_a, the weight of the soil mass in motion W and the surcharge q acting on the ground surface. Energy is dissipated at the soil-wall interface and at the lower and lateral planes between the material at rest and the material in motion.

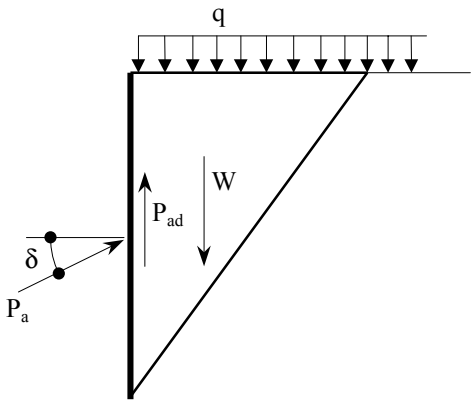

Figure 4: Free body diagram (Case I)

By equating the total rate of external work to the total rate of energy dissipation along the different velocity discontinuities, one obtains

$$P_a = K_{a\gamma} \cdot \gamma \cdot \frac{h^2}{2} \cdot b - K_{ac} \cdot c \cdot h \cdot b + K_{aq} \cdot q \cdot h \cdot b \qquad (4)$$

where $K_{a\gamma}$, K_{ac} and K_{aq} are the active earth pressure coefficients due to soil weight, cohesion and surcharge loading respectively. These coefficients are function of ϕ, δ and h/b.

4 NUMERICAL RESULTS

The critical active earth pressure coefficients are obtained by numerical optimisation. The numerical results have shown that the K_{ac} and K_{aq} coefficients are related by the following relationship (see theorem of corresponding states of Caquot and Kérisel[2]):

$$K_{ac} = \frac{\frac{1}{\cos\delta} - K_{aq}}{\tan\phi} \tag{5}$$

Thus, in the following sections, only $K_{a\gamma}$ and K_{aq} coefficients will be presented; K_{ac} may be computed using equation (5).

Figure (5) shows the variation of both $K_{a\gamma}$ and K_{aq} with h/b when $\phi=30°$ and $\delta/\phi=1$.

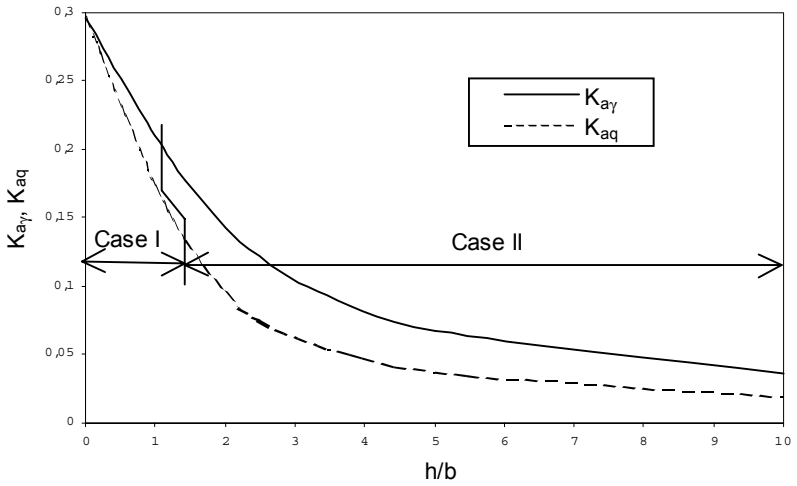

Figure 5: $K_{a\gamma}$ and K_{aq} versus h/b for $\phi=30°$ and $\delta/\phi=1$

It can be easily shown that as the length h/b increases, the active earth pressure coefficients decrease. It should be emphasised that when two-dimensional problems (i.e. small values of h/b) are used, the active earth pressure coefficients given by the present analysis are identical to those of two-dimensional analysis given by Chen[5]. This figure also shows the limit values of h/b which separate cases I and II.

Figure (6) shows the cross-sections through xOy and the traces in plan view of *M1* mechanism for $\phi=20°$, $30°$ *and* $40°$, $\delta/\phi=0$ and for two values of h/b ($h/b=1$ *and* 2.5). The value $h/b=1$ corresponds to Case I where the lateral planes do not intersect and $h/b=2.5$ corresponds to Case II where the trace of the failure mechanism in plan view is a triangle.

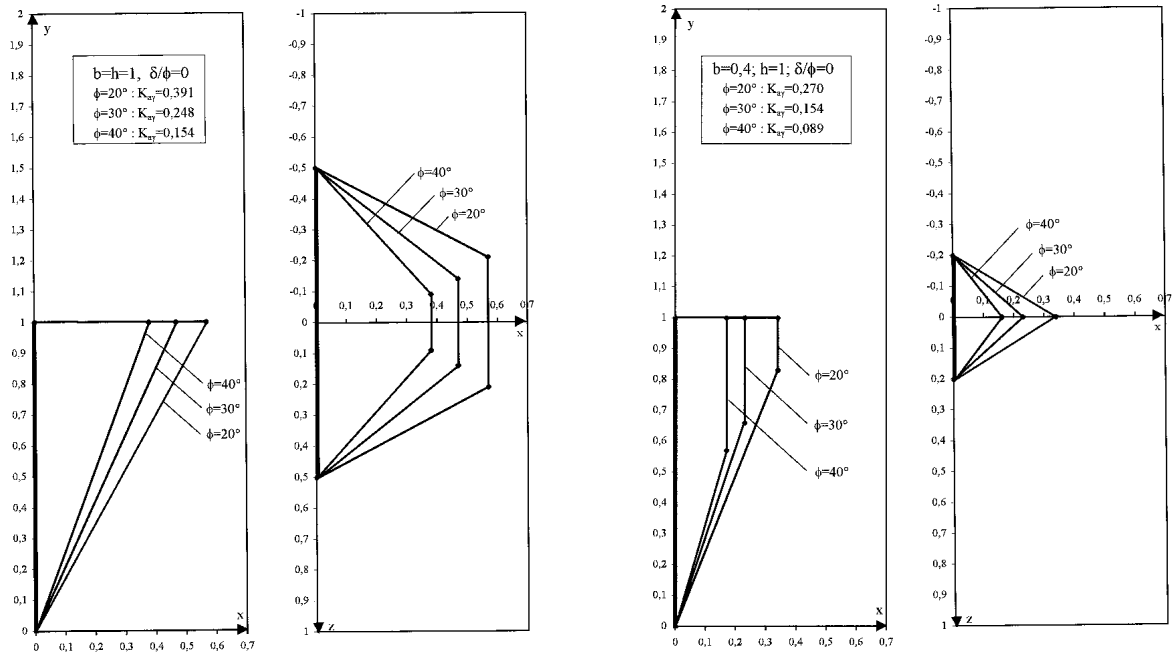

Figure 6: Cross-sections and traces in plan view of *M1* mechanism for ϕ=20°, 30° and 40° when δ/ϕ=0 and *h/b=1* and *2.5*.

Table 1 and table 2 [cf. Appendix] show some values of $K_{a\gamma}$ and K_{aq} coefficients for various governing parameters ϕ, δ and *h/b* for practical use in geotechnical engineering. As expected, the active earth pressure coefficients decrease with increasing ϕ, δ and *h/b*.

5 CONCLUSIONS

A one block translational kinematically admissible failure mechanism has been considered for the calculation of the three-dimensional active earth pressures acting on rigid retaining walls of limited breadth. The method used is the kinematical approach of the limit analysis theory. It is shown that the three dimensional active earth pressure coefficients decrease with increasing ϕ, δ and *h/b*. Two design tables relating the active earth pressure coefficients to various governing parameters ϕ, δ and *h/b* are given for practical use in geotechnical engineering.

REFERENCES

[1] Coulomb, C.A., "Sur une application des règles de maximis et minimis à quelques problèmes de statique relatifs à l'architecture", *Acad. R. Sci. Mém. Math. Phys.*, **7**, 343-382, (1773).

[2] Caquot, A., and Kérisel., J., *Traité de mécanique des sols,* Gauthier-Villars, Paris, (1949).

[3] Sokolovski, V.V., *Static of granular media,* Butterworth, London, (1960).

[4] Chen, W.F., and Rosenfarb, J.L., "Limit analysis solutions of earth pressure problems",

Soils and Foundations, **13**(4), 45-60, (1973).
[5] Chen, W.F., *Limit analysis and soil plasticity,* Elsevier, Amsterdam, 637p, (1975).
[6] Collins, I.F., "The upper-bound theorem for rigid/plastic solids to include Coulomb friction.", *J. Mech. Phys. Solids*, **17**, 323-338, (1969).
[7] Mroz, Z., and Drescher, A., "Limit plasticity approach to some cases of flow of bulk solids", *J. Engng. Ind. Trans. Am. Soc. Mech. Engrs.*, **91**, 357-364, (1969).
[8] Drescher, A., and Detournay, E., "Limit load in translational failure mechanisms for associative and non-associative materials", *Géotechnique*, **43**(3), 443-456, (1993).
[9] Michalowski, R.L., Closure on "Stability of uniformly reinforced slopes", *J. Geotech. and Geoenv. Engrg., ASCE*, **125**(1), 81-86, (1999).
[10] Soubra, A.-H., "Static and seismic passive earth pressure coefficients on rigid retaining structures", *Canadian Geotechnical Journal*, in press, (2000).

APPENDIX

		δ/ϕ				
$K_{a\gamma}$	ϕ	0	1/3	1/2	2/3	1
	10	0.41	0.37	0.36	0.35	0.33
	15	0.27	0.25	0.24	0.23	0.21
	20	0.19	0.17	0.16	0.16	0.15
h/b=4	25	0.14	0.13	0.12	0.11	0.11
	30	0.11	0.09	0.09	0.09	0.08
	35	0.08	0.07	0.07	0.07	0.06
	40	0.06	0.05	0.05	0.05	0.05
	45	0.05	0.04	0.04	0.04	0.04
	10	0.54	0.51	0.49	0.48	0.46
	15	0.40	0.37	0.36	0.35	0.33
	20	0.31	0.28	0.27	0.26	0.24
h/b=2	25	0.23	0.21	0.20	0.19	0.18
	30	0.18	0.16	0.15	0.15	0.14
	35	0.14	0.12	0.12	0.11	0.11
	40	0.10	0.09	0.09	0.09	0.09
	45	0.08	0.07	0.07	0.07	0.07
	10	0.62	0.59	0.57	0.56	0.54
	15	0.49	0.46	0.44	0.43	0.42
	20	0.39	0.36	0.35	0.34	0.33
h/b=1	25	0.31	0.28	0.28	0.27	0.26
	30	0.25	0.23	0.22	0.21	0.21
	35	0.20	0.18	0.17	0.17	0.17
	40	0.15	0.14	0.14	0.14	0.14
	45	0.12	0.11	0.11	0.11	0.12
	10	0.66	0.63	0.62	0.61	0.59
	15	0.54	0.50	0.49	0.48	0.47
	20	0.44	0.41	0.40	0.39	0.37
h/b=0.5	25	0.36	0.33	0.32	0.31	0.31
	30	0.29	0.27	0.26	0.25	0.23
	35	0.23	0.21	0.21	0.21	0.21
	40	0.18	0.17	0.17	0.17	0.17
	45	0.14	0.13	0.13	0.13	0.14
	10	0.69	0.66	0.64	0.63	0.62
	15	0.57	0.54	0.52	0.51	0.50
	20	0.47	0.44	0.43	0.42	0.41
h/b=0.2	25	0.39	0.36	0.35	0.34	0.34
	30	0.32	0.29	0.28	0.28	0.28
	35	0.26	0.24	0.23	0.23	0.23
	40	0.20	0.19	0.19	0.19	0.20
	45	0.16	0.15	0.15	0.15	0.16
	10	0.70	0.67	0.66	0.65	0.63
	15	0.59	0.56	0.54	0.53	0.52
	20	0.49	0.46	0.45	0.44	0.43
strip	25	0.41	0.38	0.37	0.36	0.35
	30	0.33	0.31	0.30	0.30	0.30
	35	0.27	0.25	0.25	0.24	0.25
	40	0.22	0.20	0.20	0.20	0.21
	45	0.17	0.16	0.16	0.16	0.18

Table 1: $K_{a\gamma}$ values for various governing parameters ϕ, δ and *h/b*.

		δ/ϕ				
K_{aq}	ϕ	0	1/3	1/2	2/3	1
	10	0.30	0.27	0.25	0.24	0.23
	15	0.18	0.16	0.15	0.14	0.13
	20	0.12	0.10	0.10	0.10	0.09
h/b=4	**25**	0.09	0.07	0.07	0.07	0.06
	30	0.06	0.05	0.05	0.05	0.05
	35	0.05	0.04	0.04	0.04	0.04
	40	0.03	0.03	0.03	0.03	0.03
	45	0.03	0.02	0.02	0.02	0.02
	10	0.47	0.44	0.42	0.41	0.39
	15	0.33	0.30	0.29	0.28	0.26
	20	0.24	0.21	0.20	0.19	0.18
h/b=2	**25**	0.17	0.15	0.14	0.13	0.13
	30	0.13	0.11	0.10	0.10	0.09
	35	0.10	0.08	0.08	0.08	0.07
	40	0.07	0.06	0.06	0.06	0.06
	45	0.05	0.05	0.04	0.04	0.05
	10	0.58	0.55	0.53	0.52	0.50
	15	0.45	0.41	0.40	0.39	0.37
	20	0.35	0.32	0.31	0.30	0.28
h/b=1	**25**	0.27	0.24	0.24	0.23	0.22
	30	0.21	0.19	0.18	0.18	0.17
	35	0.16	0.15	0.14	0.14	0.14
	40	0.13	0.11	0.11	0.11	0.11
	45	0.10	0.09	0.09	0.09	0.09
	10	0.64	0.61	0.59	0.58	0.56
	15	0.51	0.48	0.47	0.46	0.44
	20	0.41	0.38	0.37	0.36	0.35
h/b=0.5	**25**	0.33	0.31	0.30	0.29	0.28
	30	0.27	0.25	0.24	0.23	0.23
	35	0.21	0.20	0.19	0.19	0.19
	40	0.17	0.15	0.15	0.15	0.16
	45	0.13	0.12	0.12	0.12	0.13
	10	0.68	0.65	0.63	0.62	0.61
	15	0.56	0.52	0.51	0.50	0.49
	20	0.46	0.43	0.42	0.41	0.40
h/b=0.2	**25**	0.38	0.35	0.34	0.33	0.33
	30	0.31	0.28	0.28	0.27	0.27
	35	0.25	0.23	0.22	0.22	0.22
	40	0.20	0.18	0.18	0.18	0.19
	45	0.16	0.14	0.14	0.14	0.16
	10	0.70	0.67	0.66	0.65	0.63
	15	0.59	0.56	0.54	0.53	0.52
	20	0.49	0.46	0.45	0.44	0.43
strip	**25**	0.41	0.38	0.37	0.36	0.35
	30	0.33	0.31	0.30	0.30	0.30
	35	0.27	0.25	0.25	0.24	0.25
	40	0.22	0.20	0.20	0.20	0.21
	45	0.17	0.16	0.16	0.16	0.18

Table 2: K_{aq} values for various governing parameters ϕ, δ and *h/b*.